

Simple soluble molecular ionization model

Gerald V. Dunne and Christopher S. Gauthier

Department of Physics, University of Connecticut, Storrs, Connecticut 06269-3046, USA

(Received 11 February 2004; published 14 May 2004)

We present a simple exact analytical solution, using the Weyl-Titchmarsh-Kodaira spectral theorem, for the spectral function of the one-dimensional diatomic molecule model consisting of two attractive δ -function wells in the presence of a static external electric field. For sufficiently deep and far apart wells, this molecule supports both an even and an odd state, and the introduction of a static electric field turns these bound states into quasibound states which are Stark-shifted and broadened. The continuum spectrum also inherits an intricate pattern of resonances which reflect the competition between resonant scattering between the two atomic wells and between the linear potential and one or both atomic well(s). All results are analytic and can be easily plotted. The relation between the large orders of the divergent perturbative Stark-shift series and the nonperturbative widths of quasibound levels is studied.

DOI: 10.1103/PhysRevA.69.053409

PACS number(s): 42.50.Hz, 31.15.-p

I. INTRODUCTION

The electronic structure of atoms and molecules is usefully probed by external electric and magnetic fields. The development of intense lasers has permitted such probing in regimes where simple perturbative treatments are not valid and one must use a nonperturbative semiclassical approximation or a numerical approach. Experiments with molecules display a much richer range of phenomena than with atoms, due to the additional molecular degrees of freedom [1–3]. These include above-threshold ionization [4,5], multiple ionization [6,7], alignment effects [8], electron localization [9], nonsequential double ionization [10], direct excitation [11], stabilization [12], dissociative recombination [13], and separation effects [14]. However, molecules (even the simplest diatomic molecules) and their ionization are clearly more difficult to treat theoretically. Many approximation techniques have been developed and applied to atomic ionization processes [15–19], but much less is known for molecular systems. Realistic calculations are rather complicated and one loses some of the physical intuition that can often be gained from simple models. In this paper, we present the exact analytical solution for a simple molecular ionization model. The molecule is taken to be one-dimensional. This approximation is remarkably good in the strong-field regime where the ionization is predominantly along the field direction, so that the system is effectively one-dimensional [8]. The simplest such one-dimensional molecule consists of two atomic wells¹ represented by attractive δ -function wells of strength g , separated by a distance $2a$. This is a well-known soluble model [20]. This molecule always supports an even-parity bound ground state and a continuum, and if $ag > 1$ it also supports an odd-parity bound excited state. There is a long tradition of using model potentials such as zero-range potentials in atomic and molecular physics [21]. The presence of an external electrostatic field, of field strength F ,

dramatically changes the basic character of the spectrum, converting the bound states into quasibound states and modifying the resonance structure of the continuum. These spectral changes are seen directly in the spectral function $\rho(E)$: the quasibound states are poles of $\rho(E)$ at complex values of the energy E , where the real part of the pole gives the energy location of the quasibound level and the imaginary part gives the width, and hence lifetime, of the level. Since this molecular ionization model is exactly soluble, we can easily investigate the dependence of these quasibound levels on the relevant physical parameters—the field strength F , the atomic well depth g , and the atomic separation parameter a . The same applies for the “continuum,” where resonance structures appear due to the delicate interplay between tunneling, binding, and scattering effects.

The solution presented here uses the Weyl-Titchmarsh-Kodaira (WTK) spectral theorem [22–25]. This spectral theorem expresses the completeness of the wave functions of the Schrödinger equation in a general way that applies not just to the familiar discrete spectrum models (such as the infinite square well or the harmonic oscillator), but also to systems with discrete and continuum spectra (such as the finite square well or the hydrogen atom), and even to systems with a purely continuous spectrum, such as for ionization problems where there are no true bound states. The WTK approach is well suited for numerical implementation and has been applied long ago to the Stark effect in atomic hydrogen [26]. An interesting soluble one-dimensional atomic model consisting of a single finite square well on the half-line is solved using the WTK method in [27]. More recently, the numerical WTK approach has been used for studying strong-field ionization effects in effectively one-dimensional diatomic molecules [28,14]. Various numerical and approximate methods for computing resonance locations and widths are compared in [29]. This current paper is complementary to [28], but the choice to represent the atomic wells by δ -function wells makes the entire molecular ionization problem analytically solvable, thereby bypassing the numerical part of the computation. We also mention that this one-dimensional molecular ionization model has been studied in

¹It is straightforward to generalize the exact solution to the case of unequal atomic well depths, but for simplicity here we consider the atomic well depths to be equal.

[30] using the solution of the associated Lippman-Schwinger equation, and by Korsch and Mossmann [31] in terms of Stark resonances and geometric phases.

This paper is organized as follows. Section II contains a summary of the implementation of the WTK method for computing the spectral function. This is applied in Sec. III to the one-dimensional molecular model without an applied electric field. In Sec. IV the electric field is applied and the exact solution for the spectral function is derived. The dependence of the spectral function on the various physical parameters is explored through plots and also analytically. Section V is devoted to the simpler case of atomic ionization, obtained from the molecular solution by taking the atomic separation parameter, a , to zero. The final section contains some concluding comments.

II. WEYL-TITCHMARSH-KODAIRA METHOD

The Weyl-Titchmarsh-Kodaira (WTK) spectral theorem [22–25] for quantum-mechanical Hamiltonians is very general, covering not just simple Hamiltonians like the harmonic oscillator which have only bound states, but also Hamiltonians with both bound and continuum states. It also extends to ionization problems where the spectrum is purely continuum. Indeed, in his classic book [23], Titchmarsh solves the half-line “atomic” problem of a binding δ -function potential well plus a constant electric field. This approach can be applied directly to any one-dimensional or radial Schrödinger problem. The WTK method can be summarized as follows.

Consider the Schrödinger equation (we work in units where $\hbar^2/2m=1$),

$$-\psi''(x) + V(x)\psi = E\psi(x) \quad (1)$$

on the real line $x \in (-\infty, +\infty)$. Pick some point, chosen without loss of generality to be $x=0$, and normalize the two independent solutions of Eq. (1), $u(x, E)$ and $v(x, E)$, so that their Wronskian is equal to 1 at that point by choosing

$$\begin{aligned} u(0, E) = 1, \quad u'(0, E) = 0, \\ v(0, E) = 0, \quad v'(0, E) = -1. \end{aligned} \quad (2)$$

Next, integrate (numerically or analytically) each of these solutions out towards $x=+\infty$ and $x=-\infty$, producing four functions $u_{\pm}(x, E)$, and $v_{\pm}(x, E)$. The WTK method involves constructing particular linear combinations of these functions such that these combinations are normalizable on the intervals $(0, +\infty)$ and $(-\infty, 0)$, when the energy E has a small positive imaginary part: $E \rightarrow E+i\epsilon$. Specifically, going towards the right, we construct

$$\psi_+(x, E) = u_+(x, E) + m_+(E)v_+(x, E) \quad (3)$$

such that it is normalizable on the interval $(0, +\infty)$ when the energy E has a small positive imaginary part. This determines the coefficient function $m_+(E)$. Similarly, going to the left, we construct the linear combination

$$\psi_-(x, E) = u_-(x, E) + m_-(E)v_-(x, E) \quad (4)$$

such that it is normalizable on the interval $(-\infty, 0)$ when the energy E has a small positive imaginary part. This determines the coefficient function $m_-(E)$. The spectral function, and the completeness of the wave functions, can be expressed in terms of these coefficient functions $m_{\pm}(E)$ [22–25]. For example, the spectral function is

$$\rho(E) = \lim_{\epsilon \rightarrow 0} \frac{1}{\pi} \text{Im} \left(\frac{m_+(E+i\epsilon)m_-(E+i\epsilon)+1}{m_+(E+i\epsilon)-m_-(E+i\epsilon)} \right). \quad (5)$$

This WTK method is well suited to numerical implementation for arbitrary potential wells [28]. In the models studied in this paper, the situation is even simpler since the independent solutions $u(x, E)$ and $v(x, E)$ are known in analytic form for all x ; the “integration” process simply involves applying the correct continuity and discontinuity boundary conditions at the locations of the two δ -function potentials. This will be shown in detail in Sec. IV.

III. ONE-DIMENSIONAL MOLECULAR MODEL

We first review the model without the electric field. We choose the following simple double- δ -function potential to represent the diatomic molecule:

$$V(x) = -g[\delta(x+a) + \delta(x-a)], \quad (6)$$

where $g > 0$. This potential has two binding δ -function wells located at $x = \mp a$, and chosen for simplicity to have equal strength $-g$. This problem, without an external electric field, is a standard problem in quantum mechanics courses [20]. The potential (6) always supports a bound ground state which has even parity, and if $ga > 1$ it also supports a bound excited state which has odd parity. In this section, we present the WTK solution as an introductory illustration of the method.

In the vicinity of $x=0$, the potential (6) vanishes. Thus, the two independent solutions, $u(x, E)$ and $v(x, E)$, of the Schrödinger equation (1), which satisfy the normalization conditions (2), are

$$u(x, E) = \cos(\sqrt{E}x), \quad v(x, E) = -\frac{\sin(\sqrt{E}x)}{\sqrt{E}}. \quad (7)$$

Integrating to the right, these solutions remain valid until we reach the right-hand δ function at $x=+a$, at which point we impose the standard boundary conditions [20],

$$\psi(a-\epsilon) = \psi(a+\epsilon), \quad \left. \frac{d\psi}{dx} \right|_{a-\epsilon}^{a+\epsilon} = -g\psi(a). \quad (8)$$

These conditions determine the solutions for $x > a$ to be

$$u_+(x, E) = A \cos(\sqrt{E}x) + B \frac{\sin(\sqrt{E}x)}{\sqrt{E}}, \quad (9)$$

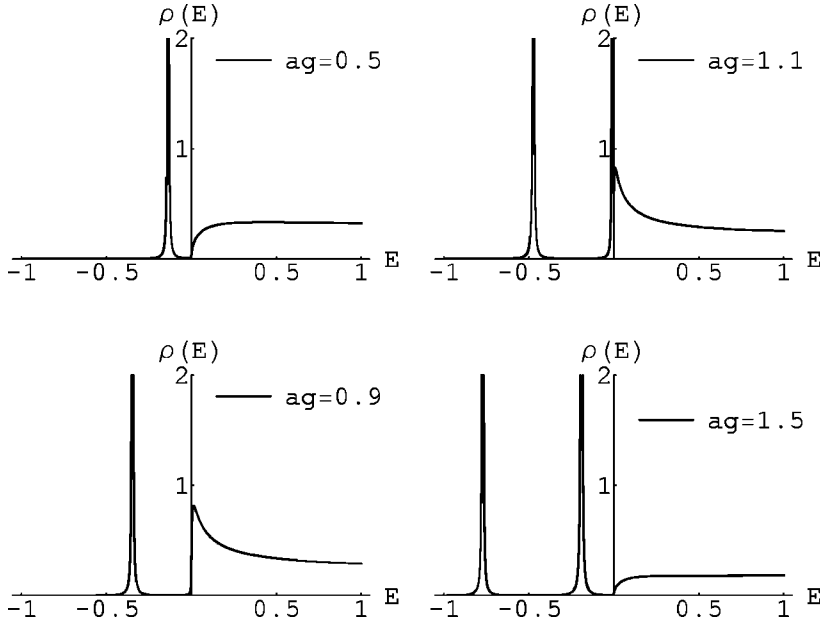


FIG. 1. Plots of the spectral function for the free one-dimensional molecular potential (6). For $ag < 1$ there is only one bound state, but for $ag > 1$ there are two bound states.

$$v_+(x, E) = C \cos(\sqrt{E}x) + D \frac{\sin(\sqrt{E}x)}{\sqrt{E}}, \quad (10)$$

$$\rho(E) = \lim_{\epsilon \rightarrow 0} \frac{1}{2\pi} \text{Im} \left(-m_+(E + i\epsilon) + \frac{1}{m_+(E + i\epsilon)} \right). \quad (14)$$

where the coefficients are

$$A = 1 + \frac{g \sin(2a\sqrt{E})}{2\sqrt{E}}, \quad B = -g \cos^2(a\sqrt{E}), \quad (11)$$

$$1 + e^{-2a\sqrt{-E}} = \frac{2\sqrt{-E}}{g}, \quad (15)$$

$$C = -\frac{g}{E} \sin^2(a\sqrt{E}), \quad D = -1 + \frac{g \sin(2a\sqrt{E})}{2\sqrt{E}}. \quad (12)$$

Bound states appear on the negative real energy axis as poles of the spectral function (14). The pole of m_+ , satisfying the transcendental equation

corresponds to the even-parity bound state. From Eq. (14), the zero of m_+ , satisfying the transcendental equation

$$1 - e^{-2a\sqrt{-E}} = \frac{2\sqrt{-E}}{g}, \quad (16)$$

When the energy E has a small positive imaginary part, the linear combination $\psi_+ = u_+ + m_+ v_+$ in Eq. (3) will be normalizable on $(0, +\infty)$ if the $\exp(-i\sqrt{E}x)$ part is eliminated. This determines the function $m_+(E)$ in Eq. (3) to be

$$m_+(E) = -\frac{\sqrt{EA} + iB}{\sqrt{EC} + iD} = \frac{-iE - g\sqrt{E} \cos(a\sqrt{E}) e^{ia\sqrt{E}}}{\sqrt{E} - g \sin(a\sqrt{E}) e^{ia\sqrt{E}}}. \quad (13)$$

also gives a pole of the spectral function, and corresponds to the odd-parity bound state (if it exists). There is always an even bound state, given by the pole of $m_+(E)$ satisfying Eq. (15). If $ga > 1$, there is also an odd bound state, given by the zero of $m_+(E)$ satisfying (16). Some plots of the spectral function (14) are shown in Figs. 1 and 2. Note the appearance of the single bound state when $ga < 1$, but of two bound states when $ga > 1$. In Fig. 1, the width of the bound state peaks in these plots is artificial, as we have kept the small imaginary part ϵ of the energy nonzero in order to show the peaks. In the true $\epsilon \rightarrow 0$ limit, these bound state peaks have zero width, and so would not show up on the plot. Figure 2

Since the potential (6) is symmetric, it follows that $m_-(E) = -m_+(E)$. Thus, the spectral function (5) is determined to be

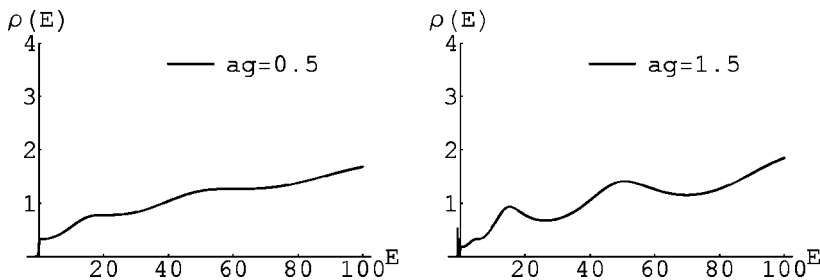


FIG. 2. Plots of the continuum part of the spectral function for the free one-dimensional molecular potential (6). Note the periodic behavior due to resonant back-scattering between the two wells. The left-hand plot is for $ag=0.5$, while the right-hand plot has $ag=1.5$.

shows the continuum part of the spectrum—notice the periodic behavior of the spectral function, due to resonant back-scattering between the two δ functions. This periodicity is determined by the separation $2a$ between the wells and the well strength g .

IV. ONE-DIMENSIONAL MOLECULAR MODEL WITH AN ELECTRIC FIELD

In this section, we solve the problem of the one-dimensional molecular potential (6) studied in the previous section, with an additional external static electric field of magnitude F . Thus, the potential is

$$V(x) = -g[\delta(x+a) + \delta(x-a)] - Fx, \quad (17)$$

where $g > 0$ and $F > 0$. The potential (17) has no bound states when $F \neq 0$, but it does have quasibound states. The corresponding Schrödinger equation (1) is analytically soluble since the linearly independent solutions are Airy functions. In fact, the WTK solution proceeds exactly as in the case without the electric field, except that the basic trigonometric solutions in Eq. (7) are replaced by Airy functions.

A. WTK solution for the spectral function

In the vicinity of $x=0$, the independent solutions satisfying the Wronskian normalization condition (2) are

$$\begin{aligned} u(x, E) &= A^{(u)} \text{Ai}\left(-\frac{Fx+E}{F^{2/3}}\right) + B^{(u)} \text{Bi}\left(-\frac{Fx+E}{F^{2/3}}\right), \\ v(x, E) &= A^{(v)} \text{Ai}\left(-\frac{Fx+E}{F^{2/3}}\right) + B^{(v)} \text{Bi}\left(-\frac{Fx+E}{F^{2/3}}\right), \end{aligned} \quad (18)$$

where Ai and Bi are Airy functions [32], and the coefficients needed to satisfy the normalization conditions (2) are

$$A^{(u)}(E) = \pi \text{Bi}'\left(-\frac{E}{F^{2/3}}\right),$$

$$B^{(u)}(E) = -\pi \text{Ai}'\left(-\frac{E}{F^{2/3}}\right),$$

$$A^{(v)}(E) = -\pi F^{-1/3} \text{Bi}\left(-\frac{E}{F^{2/3}}\right),$$

$$B^{(v)}(E) = \pi F^{-1/3} \text{Ai}\left(-\frac{E}{F^{2/3}}\right). \quad (19)$$

Here we have made use of the fundamental Airy function Wronskian identity [32],

$$\text{Ai}(x)\text{Bi}'(x) - \text{Ai}'(x)\text{Bi}(x) = \frac{1}{\pi}, \quad \forall x \in \mathbb{R}. \quad (20)$$

As before, integrating to the right, the solutions in Eqs. (18) remain valid until we reach the right-hand δ -function well at $x=+a$, at which point we apply the δ -function boundary conditions (8). This determines the solutions in the region $x > a$ to be

$$\begin{aligned} u_+(x, E) &= A_+^{(u)} \text{Ai}\left(-\frac{Fx+E}{F^{2/3}}\right) + B_+^{(u)} \text{Bi}\left(-\frac{Fx+E}{F^{2/3}}\right), \\ v_+(x, E) &= A_+^{(v)} \text{Ai}\left(-\frac{Fx+E}{F^{2/3}}\right) + B_+^{(v)} \text{Bi}\left(-\frac{Fx+E}{F^{2/3}}\right), \end{aligned} \quad (21)$$

where the coefficients are

$$\begin{aligned} A_+^{(u)}(E) &= -g\pi^2 F^{-1/3} \text{Ai}\left(-\frac{(E+Fa)}{F^{2/3}}\right) \text{Bi}\left(-\frac{(E+Fa)}{F^{2/3}}\right) \text{Bi}'\left(-\frac{E}{F^{2/3}}\right) + g\pi^2 F^{-1/3} \text{Bi}\left(-\frac{(E+Fa)}{F^{2/3}}\right)^2 \text{Ai}'\left(-\frac{E}{F^{2/3}}\right) + \pi \text{Bi}'\left(-\frac{E}{F^{2/3}}\right), \\ B_+^{(u)}(E) &= -g\pi^2 F^{-1/3} \text{Ai}\left(-\frac{(E+Fa)}{F^{2/3}}\right) \text{Bi}\left(-\frac{(E+Fa)}{F^{2/3}}\right) \text{Ai}'\left(-\frac{E}{F^{2/3}}\right) + g\pi^2 F^{-1/3} \text{Ai}\left(-\frac{(E+Fa)}{F^{2/3}}\right)^2 \text{Bi}'\left(-\frac{E}{F^{2/3}}\right) - \pi \text{Ai}'\left(-\frac{E}{F^{2/3}}\right), \\ A_+^{(v)}(E) &= g\pi^2 F^{-2/3} \text{Ai}\left(-\frac{(E+Fa)}{F^{2/3}}\right) \text{Bi}\left(-\frac{(E+Fa)}{F^{2/3}}\right) \text{Bi}\left(-\frac{E}{F^{2/3}}\right) - g\pi^2 F^{-2/3} \text{Bi}\left(-\frac{(E+Fa)}{F^{2/3}}\right)^2 \text{Ai}\left(-\frac{E}{F^{2/3}}\right) - \pi F^{-1/3} \text{Bi}\left(-\frac{E}{F^{2/3}}\right), \\ B_+^{(v)}(E) &= g\pi^2 F^{-2/3} \text{Ai}\left(-\frac{(E+Fa)}{F^{2/3}}\right) \text{Bi}\left(-\frac{(E+Fa)}{F^{2/3}}\right) \text{Ai}\left(-\frac{E}{F^{2/3}}\right) - g\pi^2 F^{-2/3} \text{Ai}\left(-\frac{(E+Fa)}{F^{2/3}}\right)^2 \text{Bi}\left(-\frac{E}{F^{2/3}}\right) + \pi F^{-1/3} \text{Ai}\left(-\frac{E}{F^{2/3}}\right). \end{aligned} \quad (22)$$

Similarly, integrating to the left, the solutions (18) remain valid until we reach the left-hand δ function well at $x=-a$, at which point we apply the boundary conditions (8). This determines the solutions in the region $x < -a$ to be

$$\begin{aligned}
u_-(x,E) &= A_-^{(u)} \text{Ai}\left(-\frac{(Fx+E)}{F^{2/3}}\right) + B_-^{(u)} \text{Bi}\left(-\frac{(Fx+E)}{F^{2/3}}\right), \\
v_-(x,E) &= A_-^{(v)} \text{Ai}\left(-\frac{(Fx+E)}{F^{2/3}}\right) + B_-^{(v)} \text{Bi}\left(-\frac{(Fx+E)}{F^{2/3}}\right),
\end{aligned} \tag{23}$$

where the coefficients are

$$\begin{aligned}
A_-^{(u)}(E) &= g\pi^2 F^{-1/3} \text{Bi}\left(-\frac{(E-Fa)}{F^{2/3}}\right) \text{Ai}\left(-\frac{(E-Fa)}{F^{2/3}}\right) \text{Bi}'\left(-\frac{E}{F^{2/3}}\right) - g\pi^2 F^{-1/3} \text{Bi}\left(-\frac{(E-Fa)}{F^{2/3}}\right)^2 \text{Ai}'\left(-\frac{E}{F^{2/3}}\right) + \pi \text{Bi}'\left(-\frac{E}{F^{2/3}}\right), \\
B_-^{(u)}(E) &= g\pi^2 F^{-1/3} \text{Bi}\left(-\frac{(E-Fa)}{F^{2/3}}\right) \text{Ai}\left(-\frac{(E-Fa)}{F^{2/3}}\right) \text{Ai}'\left(-\frac{E}{F^{2/3}}\right) - g\pi^2 F^{-1/3} \text{Ai}\left(-\frac{(E-Fa)}{F^{2/3}}\right)^2 \text{Bi}'\left(-\frac{E}{F^{2/3}}\right) - \pi \text{Ai}'\left(-\frac{E}{F^{2/3}}\right), \\
A_-^{(v)}(E) &= -g\pi^2 F^{-2/3} \text{Bi}\left(-\frac{(E-Fa)}{F^{2/3}}\right) \text{Ai}\left(-\frac{(E-Fa)}{F^{2/3}}\right) \text{Bi}\left(-\frac{E}{F^{2/3}}\right) + g\pi^2 F^{-2/3} \text{Bi}\left(-\frac{(E-Fa)}{F^{2/3}}\right)^2 \text{Ai}\left(-\frac{E}{F^{2/3}}\right) - \pi F^{-1/3} \text{Bi}\left(-\frac{E}{F^{2/3}}\right), \\
B_-^{(v)}(E) &= -g\pi^2 F^{-2/3} \text{Bi}\left(-\frac{(E-Fa)}{F^{2/3}}\right) \text{Ai}\left(-\frac{(E-Fa)}{F^{2/3}}\right) \text{Ai}\left(-\frac{E}{F^{2/3}}\right) + g\pi^2 F^{-2/3} \text{Ai}\left(-\frac{(E-Fa)}{F^{2/3}}\right)^2 \text{Bi}\left(-\frac{E}{F^{2/3}}\right) + \pi F^{-1/3} \text{Ai}\left(-\frac{E}{F^{2/3}}\right).
\end{aligned} \tag{24}$$

Thus, the independent solutions to the Schrödinger equation for the potential (17) are known analytically for all x . As described in Sec. II, the WTK method involves finding the functions $m_{\pm}(E)$ such that the linear combinations $\psi_{\pm} = u_{\pm} + m_{\pm} v_{\pm}$ are normalizable as $x \rightarrow \pm\infty$, when the energy has a small positive imaginary part.

In the region $x > a$, the normalizable solution has the form

$$\psi_+(x,E) \propto \text{Ai}\left(-\frac{(Fx+E)}{F^{2/3}}\right) - i \text{Bi}\left(-\frac{(Fx+E)}{F^{2/3}}\right). \tag{25}$$

This determines $m_+(E)$ to be

$$m_+(E) = -\frac{B_+^{(u)}(E) + i A_+^{(u)}(E)}{B_+^{(v)}(E) + i A_+^{(v)}(E)}. \tag{26}$$

In the region $x < -a$, the normalizable solution has the form

$$\psi_-(x,E) \propto \text{Ai}\left(-\frac{(Fx+E)}{F^{2/3}}\right). \tag{27}$$

This determines $m_-(E)$ to be

$$m_-(E) = -\frac{B_-^{(u)}(E)}{B_-^{(v)}(E)}. \tag{28}$$

Given these expressions for $m_{\pm}(E)$, the spectral function is given by Eq. (5), which we can write in terms of the coefficients (22) and (24) as

$$\rho(E) = \lim_{\epsilon \rightarrow 0} \frac{1}{\pi} \text{Im} \left(\frac{B_-^{(u)}(E+i\epsilon)[B_+^{(u)}(E+i\epsilon) + iA_+^{(u)}(E+i\epsilon)] + B_-^{(v)}(E+i\epsilon)[B_+^{(v)}(E+i\epsilon) + iA_+^{(v)}(E+i\epsilon)]}{B_-^{(u)}(E+i\epsilon)[B_+^{(v)}(E+i\epsilon) + iA_+^{(v)}(E+i\epsilon)] - B_-^{(v)}(E+i\epsilon)[B_+^{(u)}(E+i\epsilon) + iA_+^{(u)}(E+i\epsilon)]} \right). \tag{29}$$

This is an analytic expression for the exact spectral function for the potential (17). In the remainder of this section, we discuss the physical properties of this spectral function, using plots and analytical methods.

B. Plots of the spectral function

Before discussing the analytic properties of the spectral function (29), we present some plots which illustrate how the spectral function depends on the physical parameters, in order to develop some intuition for the physical processes in-

involved. In addition, some animations showing how the spectral function changes, both in the quasibound and in the quasicontinuum region, as we vary the field strength F , the atomic separation parameter a , or the atomic well depth parameter g , can be found in [33].

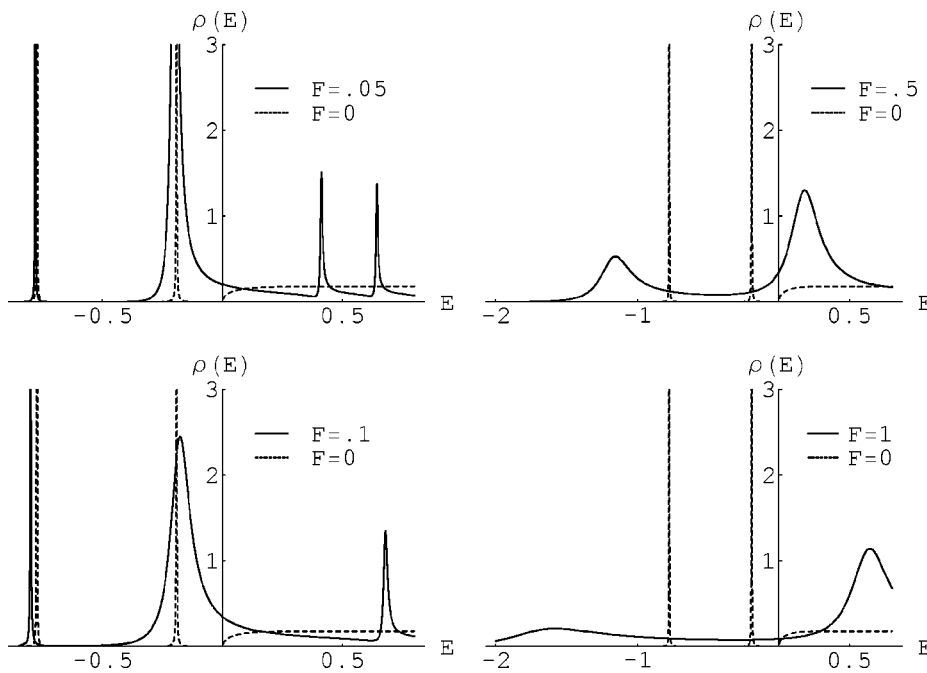


FIG. 3. Plots of the spectral function (29) (solid lines) illustrating how the quasibound states change as the electric field strength F varies. The dashed line shows the corresponding $F=0$ molecular spectrum (14). In these plots, the atomic well strength is $g=1.5$, and the separation parameter is $a=1$, so the free molecule has two bound states. Notice that as F increases, these two states are Stark-shifted and broadened.

1. Dependence on the electric field strength F

In the absence of the electric field, the molecule has one or two bound states depending on the well separation parameter a and well strength g . And the continuum exhibits structure due to Ramsauer-Townsend resonances in the scattering between the two δ wells. These two features are illustrated clearly in Figs. 1 and 2. When the field strength F is nonzero, the bound states become quasibound states with a nonzero width, and their central values are Stark-shifted. These effects are illustrated in Fig. 3, which shows a molecule with two bound states subjected to an external electric field of strengths $F=0.05, 0.1, 0.5, 1$. Note that the quasibound states

broaden as the field increases, with the higher state being broader since it is less deeply bound and so can tunnel more easily. The quasibound states are Stark-shifted in opposite directions: the lower state is Stark-shifted down in energy, while the higher state is Stark-shifted up in energy. The effect of the external electrostatic field on the continuum states is shown in Fig. 4. In these plots, the dashed line shows the continuum spectral function when $F=0$. The solid lines show the spectral function for various values of $F: F=5, 10, 15, 20$. Note that the free spectral function provides an average for the $F>0$ spectral function. The scale of the oscillations of this average function is clearly independent of

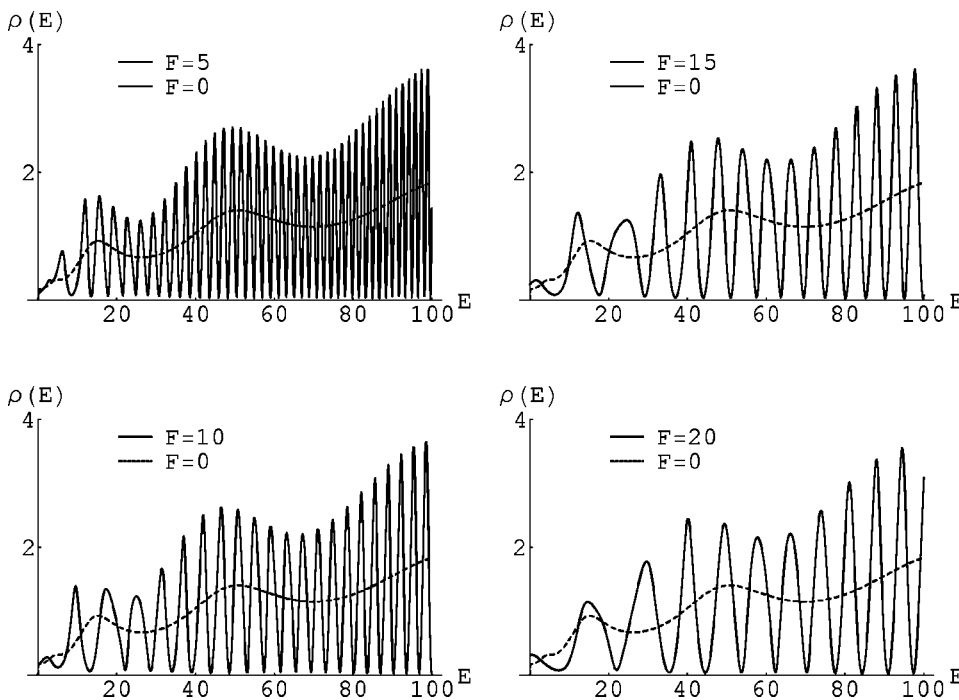


FIG. 4. Plots of the spectral function (29) (solid lines) illustrating how the continuum part of the spectrum changes as the electric field strength F varies. The dashed line shows the corresponding $F=0$ molecular spectrum (14). In these plots, the atomic well strength is $g=1.5$, and the separation parameter is $a=1$. Notice the two oscillation scales—the longer one is set by the free case (dashed line) while the rapid oscillation is set by the field strength F , with the free spectral function providing an average. As F decreases in magnitude, the oscillations become more rapid, eventually averaging out to the free case.

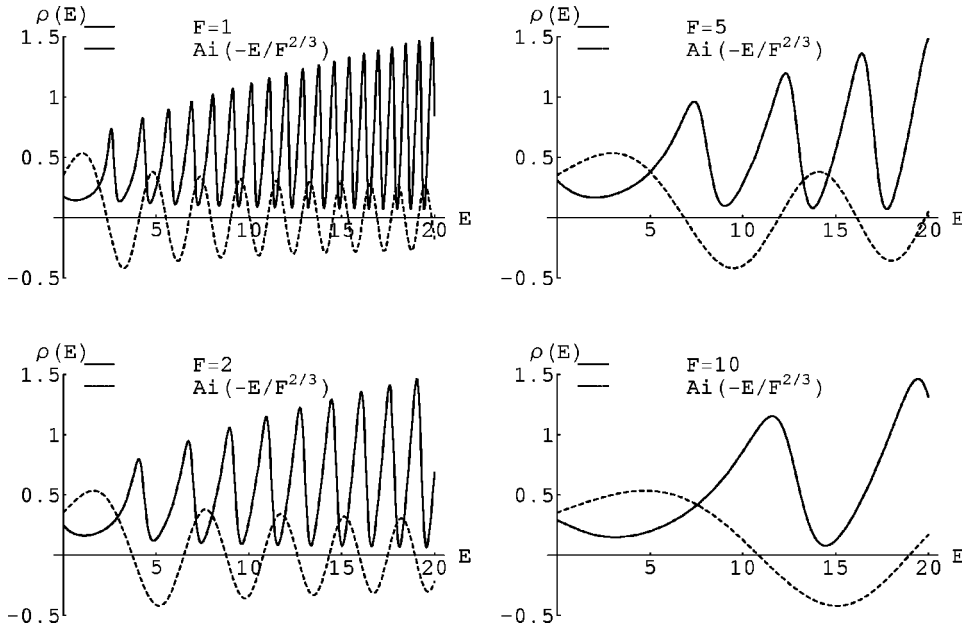


FIG. 5. Plots of the spectral function (29) (solid lines) illustrating how the continuum part of the spectrum correlates with the zeros of the Airy function $\text{Ai}(-E/F^{2/3})$ (dashed line), which are the energies of the wedge potential $V = -Fx$ with an infinite wall at some point. This is an illustration of the Ramsauer effect. These plots are for $a=0$ and $g=1$, and various values of the electric field strength F , as shown.

F , being determined by the combination ag , as illustrated in Fig. 2. For $F > 0$, there is an additional scale in the “continuum” spectrum, and as F decreases to zero the rapid oscillations become more and more rapid, and eventually average out to the free spectral function. As F increases, the period of this oscillation increases. These oscillations can be correlated approximately with the zeros of the Airy function $\text{Ai}(-E/F^{2/3})$, since these zeros give the energies of the half-wedge potential well which has $V = -Fx$ for $x < 0$, with an infinite barrier at $x = 0$. This is illustrated in Figs. 5 and 6, for $a = 0$ and $a = 1$, respectively. Note that the peaks of the spectral function (the solid line) coincide roughly with the zeros of $\text{Ai}(-E/F^{2/3})$, the dashed line. The agreement is quite good, even for the molecular model having $a = 1$. This is an example of Ramsauer-Townsend resonance, with the electron backscattering off the two δ wells providing the large-period

oscillations, and the electron scattering off the δ wells and the linear electrostatic potential providing the shorter-period oscillations.

2. Dependence on the atomic well separation parameter a

The dependence of the spectral function (29) on the atomic well separation parameter a is illustrated in Figs. 7 and 8 for the “bound” and “continuum” parts of the spectrum, respectively. In the zero-field case, the spectral function has two bound states if $ga > 1$. These are shown as the dashed curves in Fig. 7. As the separation increases, these two bound states approach the same energy, becoming degenerate in the limit $a \rightarrow \infty$. This is because in the large separation limit the tunneling which mixes the two levels becomes suppressed and the two atoms become essentially independent of one another. Thus the bound state spectrum

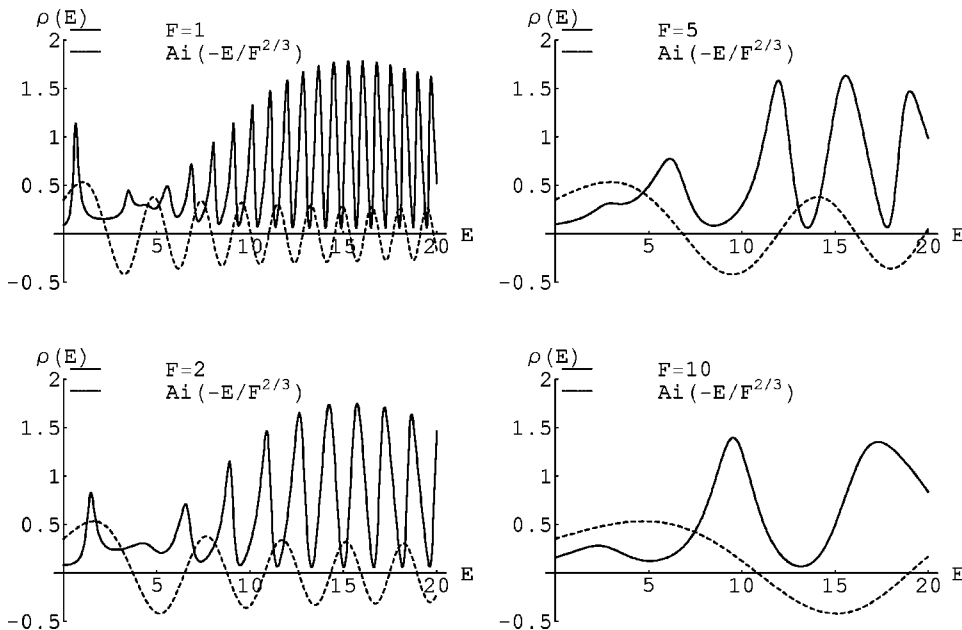


FIG. 6. Plots of the spectral function (29) (solid lines) illustrating how the continuum part of the spectrum correlates with the zeros of the Airy function $\text{Ai}(-E/F^{2/3})$ (dashed line), which are the energies of the wedge potential $V = -Fx$ with an infinite wall at some point. This is an illustration of the Ramsauer effect. These plots are for $a=1$ and $g=1.5$, and various values of the electric field strength F , as shown.

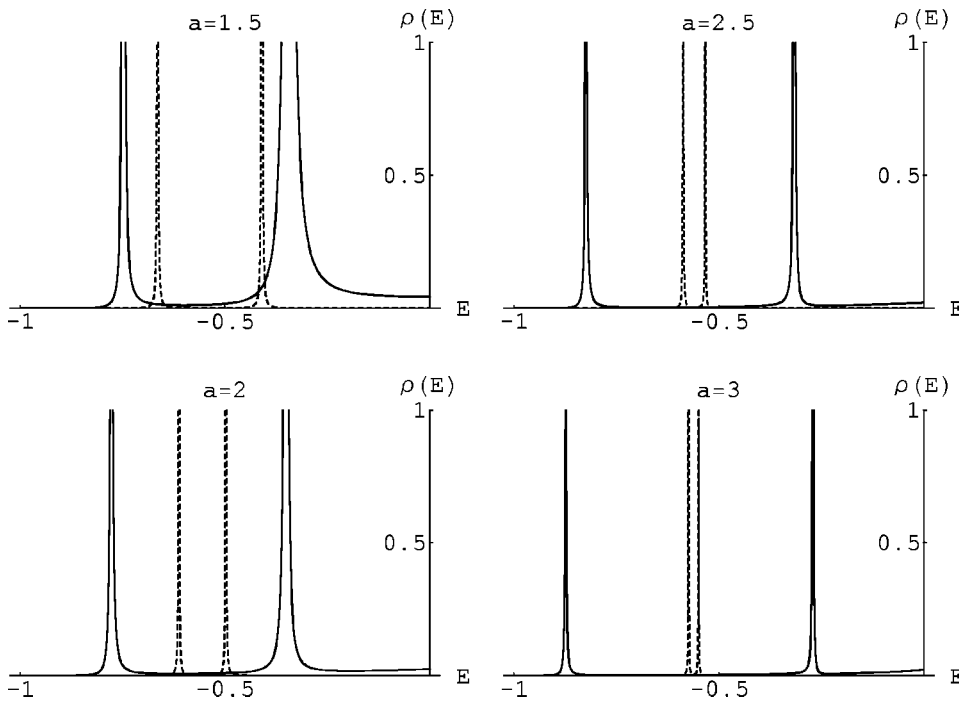


FIG. 7. Plots of the spectral function (29) (solid lines) illustrating how the quasibound part of the spectrum changes as the well separation parameter a varies. The dashed line shows the corresponding $F=0$ molecular spectrum (14). For the solid lines, the field strength is $F=0.1$, the well strength is $g=1.5$, and a ranges through 1.5, 2, 2.5, and 3. Notice that as a increases, the quasibound states become narrower in width and they move apart. In contrast, the free bound states move together, eventually becoming degenerate as $a \rightarrow \infty$.

approaches that of a single atomic well. On the other hand, if the field strength is nonzero, the quasibound states do not become degenerate in the limit of large separation. This is shown by the solid curves in Fig. 7. Instead, the two states

move away from each other; the even state is Stark-shifted further down in energy and the odd state is Stark-shifted further up in energy. This is because for large a the tunneling is essentially from each well independently, with one Stark-

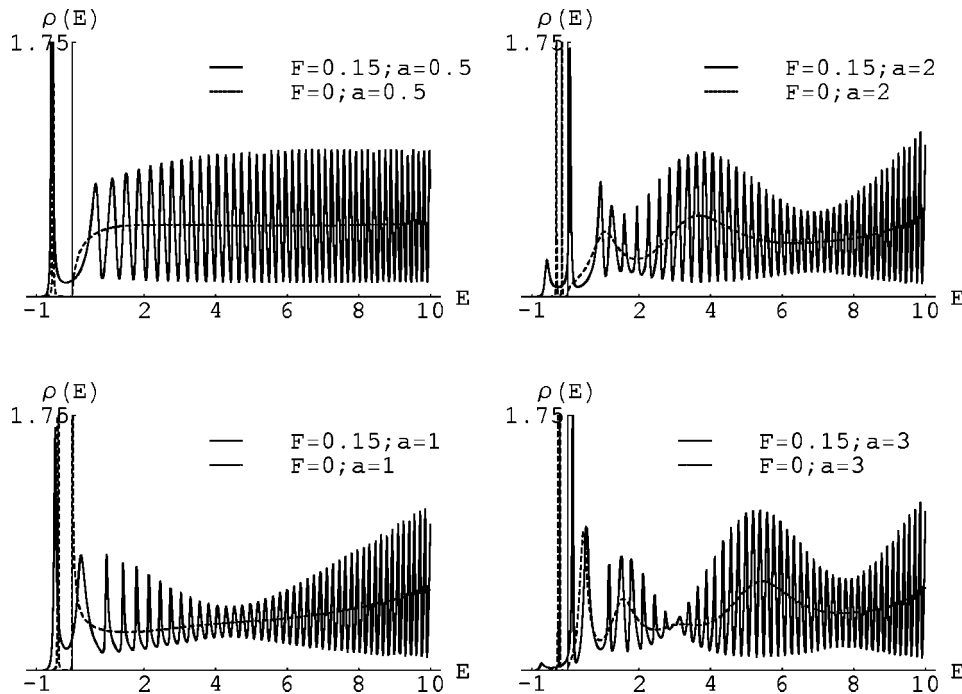


FIG. 8. Plots of the spectral function (29) (solid lines) illustrating how the continuum part of the spectrum changes as the well separation parameter a varies. The dashed line shows the corresponding $F=0$ molecular spectrum (14). In these plots, the field strength is $F=0.15$ and the well strength is $g=1$. Notice that as a increases, a second quasibound state peels off the positive energy continuum and forms a Stark-shifted pair around the two $F=0$ bound states which exist for $ag > 1$. Also note that in the $F=0$ case, as a increases the splitting between the two bound states becomes vanishingly small, as the tunneling between the two wells is suppressed. In the continuum, the average function varies with a due to resonances in the backscattering between the two wells. Even with nonzero F , the spectral function follows this average closely as a varies.

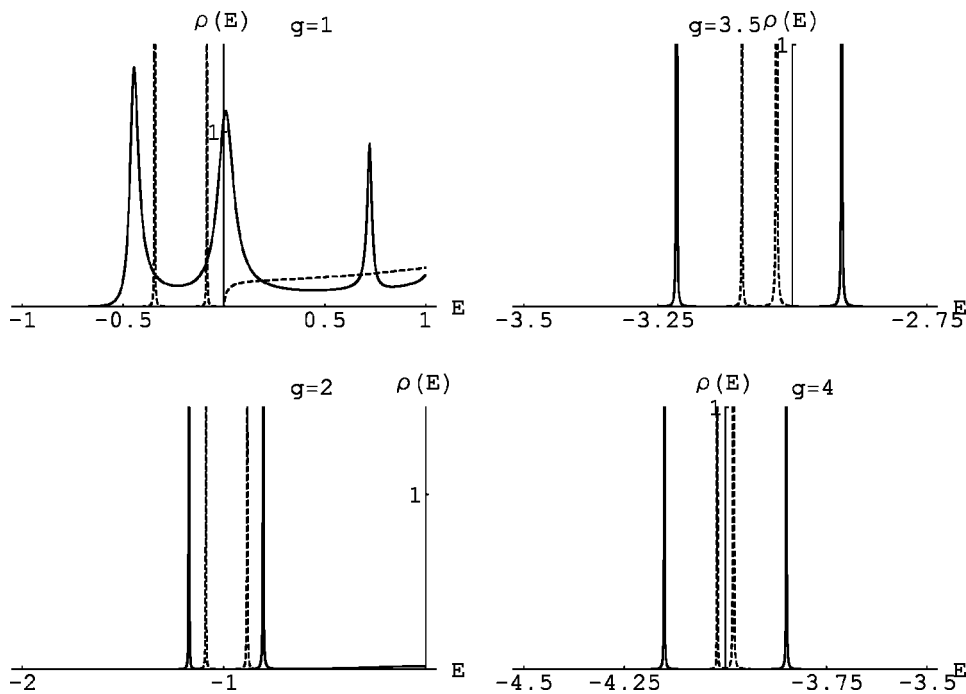


FIG. 9. Plots of the spectral function (29) (solid lines) illustrating how the quasibound part of the spectrum changes as the well depth parameter g varies. The dashed line shows the corresponding $F=0$ molecular spectrum (14). In these plots, the field strength is $F=0.1$ and the well separation parameter is $a=1.5$.

shifted up and the other down, depending on the parity of the original state. These quasibound levels also become narrower in width as there is a larger barrier through which the electron must tunnel as a increases. The effect on the “continuum” part of the spectrum is shown in Fig. 8. Here $F=0.15$ and the spectrum exhibits resonances which oscillate about the $F=0$ case, which is shown by the dashed lines. As the well separation changes, the average function changes, due to the Ramsauer-Townsend resonance between the two wells. Note that for nonzero field strength the spectral function oscillates rapidly with energy, but still follows the free field average. Thus, the $F>0$ spectral function represents a

competition between the resonance between the two wells, which depends strongly on a , and the resonance between a given well and the linear potential, which is not sensitive to a .

3. Dependence on the atomic well strength g

The dependence of the spectral function (29) on the atomic well depth g is illustrated in Fig. 9 and 10 for the “bound” and “continuum” parts of the spectrum, respectively. In the $F=0$ case, the difference in energy between the even and odd states gets smaller as the well strength increases, which is similar to what happens when the well

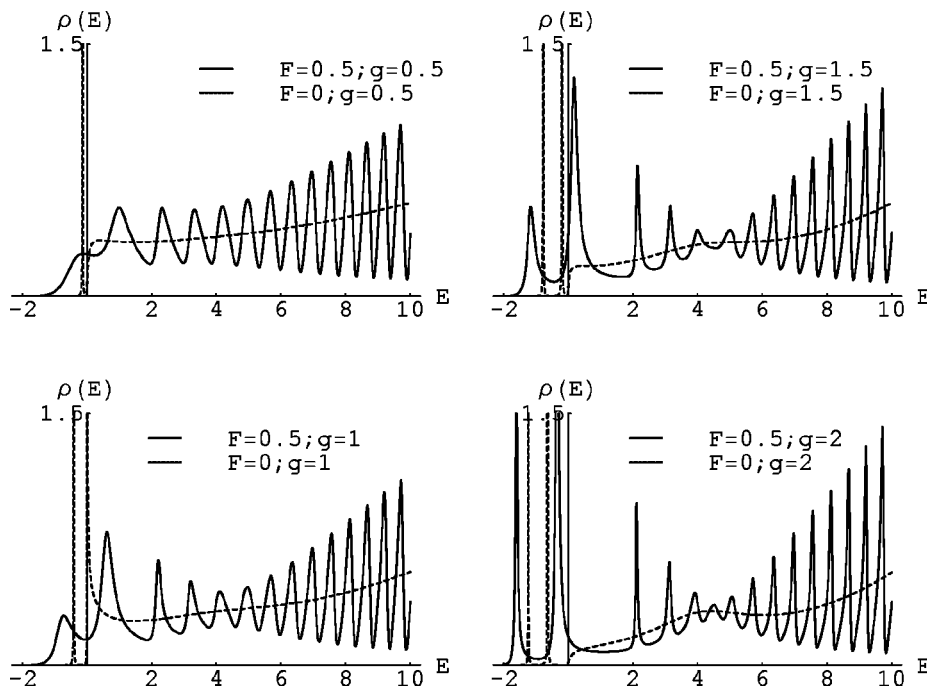


FIG. 10. Plots of the spectral function (29) (solid lines) illustrating how the continuum part of the spectrum changes as the well depth parameter g varies. The dashed line shows the corresponding $F=0$ molecular spectrum (14). In these plots, the field strength is $F=0.5$ and the well separation parameter is $a=1$. Notice that as g increases, a second quasibound state peels off the positive energy continuum and forms a Stark-shifted pair around the two $F=0$ bound states which exist for $ag>1$.

separation increases. This is because the tunneling mixing is more highly suppressed as the states become more deeply bound. The difference between the limit of large well separation and the limit of large well strength is that as the well separation increases, the two bounded states approach the same energy, whereas when the well strength is increased the states become degenerate but their energies tend to $-\infty$ as $g \rightarrow \infty$. However, if the electric field is applied, the two states do not become degenerate in the large well strength limit but instead keep a nonzero relative distance between each other. The distance between the two states approaches $2Fa$ as well strength increases, which is easily explained by the following argument. If the well strength is very strong, we can think of a particle being localized at a single well. If a uniform electric field of strength F pointing in the positive x direction is applied, a particle localized at the left well will increase in energy by Fa while the energy of a particle localized at the right well will decrease by Fa . Since the unperturbed states have the same energy, the energy difference is just $2Fa$. This can be seen in the last panels of Fig. 9, for which $F=0.1$ and $a=1.5$, so $2Fa=0.3$, which is roughly the separation between the two quasibound levels. Also note that the quasibound state peaks become narrower as g increases, as the levels are more deeply bound.

Backscattering resonances in the continuum become more prominent as the well strength increases, because the resonances are sharper, since the scattering potentials are deeper. If the field is weak, the WKB approximation for an infinite well potential in an electric field can be used to find the energies of the backscattering states in the strong-well-strength limit. But these peaks also follow the free field average (the dashed lines in Fig. 10), which is due to the resonance between the wells without the electric field. Thus, the $F > 0$ spectral function represents a competition between the resonance between the two wells, which depends strongly on g , and the resonance between a given well and the linear potential, which is also sensitive to the well strength g .

C. Analytic properties of spectral function: Stark shifts and level widths

With the electric field present there are no true bound states, but there are quasibound states. The location of these quasibound states is given by the real parts of the poles of the spectral function (29), and their widths are given by the imaginary part of these poles. These poles are given by the zeros of

$$\begin{aligned}
 & F^{-1/3} + ig^2 \pi^2 F^{-1} \text{Ai}\left(-\frac{(E-Fa)}{F^{2/3}}\right) \left\{ \left[\text{Ai}\left(-\frac{(E+Fa)}{F^{2/3}}\right) - i \text{Bi}\left(-\frac{(E+Fa)}{F^{2/3}}\right) \right] \left[\text{Ai}\left(-\frac{(E+Fa)}{F^{2/3}}\right) \text{Bi}\left(-\frac{(E-Fa)}{F^{2/3}}\right) \right. \right. \\
 & \quad \left. \left. - \text{Ai}\left(-\frac{(E-Fa)}{F^{2/3}}\right) \text{Bi}\left(-\frac{(E+Fa)}{F^{2/3}}\right) \right] \right\} - g \pi F^{-2/3} \left[i \text{Ai}\left(-\frac{(E-Fa)}{F^{2/3}}\right)^2 \right. \\
 & \quad \left. + \text{Ai}\left(-\frac{(E-Fa)}{F^{2/3}}\right) \text{Bi}\left(-\frac{(E-Fa)}{F^{2/3}}\right) + i \text{Ai}\left(-\frac{(E+Fa)}{F^{2/3}}\right)^2 + \text{Ai}\left(-\frac{(E+Fa)}{F^{2/3}}\right) \text{Bi}\left(-\frac{(E+Fa)}{F^{2/3}}\right) \right]. \quad (30)
 \end{aligned}$$

In the weak-field limit, we can use the following asymptotic expansions [32] of the Airy functions to find perturbative solutions for the zeros of Eq. (30):

$$\text{Ai}(z) \sim \frac{e^{-\zeta}}{2\sqrt{\pi z}^{1/4}} \sum_{k=0}^{\infty} \frac{(-1)^k c_k}{\zeta^k}, \quad (31)$$

$$\text{Bi}(z) \sim \frac{e^{\zeta}}{\sqrt{\pi z}^{1/4}} \sum_{k=0}^{\infty} \frac{c_k}{\zeta^k}, \quad (32)$$

where $\zeta = \frac{2}{3}z^{3/2}$, and the expansion coefficients c_k are

$$c_k = \frac{\Gamma(3k+1/2)}{54^k k! \Gamma(k+1/2)}. \quad (33)$$

Clearly, only even powers of F will appear in the perturbative expansion for the real parts of the quasienergies. So, we define the expansion

$$E = -g^2 \sum_{n=0}^{\infty} a_n \left(\frac{F}{g^3}\right)^{2n}. \quad (34)$$

To find the real parts of the quasienergies, we can ignore the imaginary parts of Eq. (30), which are anyway exponentially suppressed in the weak-field limit. It is a straightforward exercise to expand Eq. (30) in powers of the field strength F , using, for example, MATHEMATICA [37]. The leading-order F^0 term produces the equation

$$4a_0 - 4\sqrt{a_0} + (1 - e^{-4ag\sqrt{a_0}}) = 0 \quad (35)$$

whose solutions are just the solutions of the transcendental equations (15) and (16) derived in the previous section for the bound states in the free field case. A solution to Eq. (35) satisfying Eq. (15) is an even bound state of the $F=0$ potential (6), while a solution to Eq. (35) satisfying Eq. (16) is an odd bound state of Eq. (6).

The first correction to these bound states comes from the F^2 term in the expansion of Eq. (30), which leads to the following expression for a_1 in terms of a_0 :

$$a_1 = \frac{15(1 - 2\sqrt{a_0}) - 15ag(1 - 2\sqrt{a_0})^2 + 12(ag)^2a_0(1 - 4\sqrt{a_0}) - 4(ag)^3a_0(1 - 2\sqrt{a_0})^2}{48a_0^2(1 - 2\sqrt{a_0})[1 - ag(1 - 2\sqrt{a_0})]}. \quad (36)$$

Thus, to first nontrivial order, the Stark-shifted energy is

$$E = -a_0g^2 - a_1\frac{F^2}{g^4} + \dots \quad (37)$$

To find the shift for the even bound state, we find the solution a_0 of Eq. (52) which also satisfies Eq. (15), and then insert this value of a_0 into Eq. (36) to find the corresponding a_1 . It is straightforward to continue this to higher orders. For the odd bound state, we must first find if there is such a solution for a_0 to Eq. (52) satisfying Eq. (16). This odd solution will exist if $ga > 1$. If it exists, then the corresponding Stark shift is obtained by inserting this value of a_0 into the expression (36) for a_1 .

The widths of the quasibound states can be derived from the imaginary part of the poles of the spectral function. Because of the complicated dependence of the quasibound state energies on the system parameters F , g , and a , it is difficult to derive simple analytical expressions for the linewidths. However, in the large atomic separation limit, as $a \rightarrow \infty$, we can use the WKB method to approximate the tunneling rate, and hence the linewidth, as

$$\Gamma \sim g\sqrt{E_0 - Fa} \exp\left[-\frac{4(E_0 - Fa)^{3/2}}{3F}\right], \quad (38)$$

where $E = -E_0 - i\Gamma$, and $-E_0$ is the full Stark-shifted energy of the lower quasibound state.

In the limit of infinitely large well strength, $g \rightarrow \infty$, the g^2 term in Eq. (30) dominates and the zeros of Eq. (30) lie on the positive real axis. If the field strength F is small, the first-order asymptotic expansion of the Airy functions [32],

$$\text{Ai}(-z) \sim \frac{1}{\sqrt{\pi z}^{1/4}} \sin\left(\zeta + \frac{\pi}{4}\right), \quad (39)$$

$$\text{Bi}(-z) \sim \frac{1}{\sqrt{\pi z}^{1/4}} \cos\left(\zeta + \frac{\pi}{4}\right), \quad \zeta = \frac{2}{3}z^{3/2} \quad (40)$$

for $\text{Re}(z) \gg 0$ can be used to estimate the location of the zeros of Eq. (30). These approximate zeros are determined by the expressions

$$\frac{2(E - Fa)^{3/2}}{3F} = \left(n - \frac{1}{4}\right)\pi, \quad (41)$$

$$\frac{2(E + Fa)^{3/2} - (E - Fa)^{3/2}}{3F} = n\pi. \quad (42)$$

Note that expression (41) approximates the zeros of

$$\text{Ai}\left(-\frac{(E - Fa)}{F^{2/3}}\right),$$

while Eq. (42) approximates the zeros of

$$\text{Ai}\left(-\frac{(E + Fa)}{F^{2/3}}\right)\text{Bi}\left(-\frac{(E - Fa)}{F^{2/3}}\right) - \text{Ai}\left(-\frac{(E - Fa)}{F^{2/3}}\right)\text{Bi}\left(-\frac{(E + Fa)}{F^{2/3}}\right).$$

Solutions for expression (41) are the energies obtained using the WKB approximation for a half-wedge potential with an infinitely high wall at $x = -a$. Therefore, we interpret the energies satisfying Eq. (41) as those of the backscattering states between the left well and the electric field, which is the Ramsauer effect illustrated in Figs. 5 and 6. Similarly, expression (42) yields the same set of energies obtained from the WKB approximation for a potential well in an electric field with infinitely high walls at $x = -a$ and $x = a$, and therefore Eq. (42) determines the energies of backscattering states between the two wells, also in the presence of the electric field. In general, the exact resonances reflect a competition of these scatterings among the linear potential and the atomic wells.

V. SINGLE-WELL POTENTIAL WITH AN ELECTRIC FIELD

A nice feature of our molecular analysis is that the ‘‘atomic’’ analogue of the molecular model studied in Sec. IV can be obtained simply by setting the separation parameter a of the two wells to zero. All the expressions carry over smoothly in this $a \rightarrow 0$ limit. The corresponding potential is (note that the δ -function strength becomes $2g$ in this limit)

$$V(x) = -2g\delta(x) - Fx. \quad (43)$$

This atomic problem has also been discussed in terms of the corresponding Green’s functions in [34,35], and in terms of Stark resonances in [36].

WTK solution for the atomic spectral function

The spectral function is given, as before in Eq. (29), by

$$\rho(E) = \lim_{\epsilon \rightarrow 0} \frac{1}{\pi} \text{Im} \left(\frac{B_-^{(u)}(E + i\epsilon)[B_+^{(u)}(E + i\epsilon) + iA_+^{(u)}(E + i\epsilon)] + B_-^{(v)}(E + i\epsilon)[B_+^{(v)}(E + i\epsilon) + iA_+^{(v)}(E + i\epsilon)]}{B_-^{(u)}(E + i\epsilon)[B_+^{(v)}(E + i\epsilon) + iA_+^{(v)}(E + i\epsilon)] - B_-^{(v)}(E + i\epsilon)[B_+^{(u)}(E + i\epsilon) + iA_+^{(u)}(E + i\epsilon)]} \right), \quad (44)$$

where the coefficient functions in Eqs. (22) and (24) now simplify to

$$\begin{aligned}
A_+^{(u)}(E) &= \pi \left[\text{Bi}'\left(-\frac{E}{F^{2/3}}\right) - gF^{-1/3}\text{Bi}\left(-\frac{E}{F^{2/3}}\right) \right], \\
B_+^{(u)}(E) &= -\pi \left[\text{Ai}'\left(-\frac{E}{F^{2/3}}\right) - gF^{-1/3}\text{Ai}\left(-\frac{E}{F^{2/3}}\right) \right], \\
A_+^{(v)}(E) &= -\pi F^{-1/3}\text{Bi}\left(-\frac{E}{F^{2/3}}\right), \\
B_+^{(v)}(E) &= \pi F^{-1/3}\text{Ai}\left(-\frac{E}{F^{2/3}}\right), \\
A_-^{(u)}(E) &= \pi \left[\text{Bi}'\left(-\frac{E}{F^{2/3}}\right) + gF^{-1/3}\text{Bi}\left(-\frac{E}{F^{2/3}}\right) \right], \\
B_-^{(u)}(E) &= -\pi \left[\text{Ai}'\left(-\frac{E}{F^{2/3}}\right) + gF^{-1/3}\text{Ai}\left(-\frac{E}{F^{2/3}}\right) \right], \\
A_-^{(v)}(E) &= -\pi F^{-1/3}\text{Bi}\left(-\frac{E}{F^{2/3}}\right), \\
B_-^{(v)}(E) &= \pi F^{-1/3}\text{Ai}\left(-\frac{E}{F^{2/3}}\right). \tag{45}
\end{aligned}$$

Taylor expanding in ϵ leads to a more explicit expression for the spectral function,

$$\begin{aligned}
\rho(E) &= \frac{1}{\left[2\pi g F^{-2/3} \text{Ai}\left(-\frac{E}{F^{2/3}}\right) \right]^2 + \left[2\pi g F^{-2/3} \text{Bi}\left(-\frac{E}{F^{2/3}}\right) \text{Ai}\left(-\frac{E}{F^{2/3}}\right) - F^{-1/3} \right]^2} \left(\left\{ \left[(1-g^2)\pi F^{-2/3} \text{Ai}\left(-\frac{E}{F^{2/3}}\right) \text{Bi}\left(-\frac{E}{F^{2/3}}\right) \right. \right. \right. \\
&+ \left. \left. \left. \pi \text{Ai}'\left(-\frac{E}{F^{2/3}}\right) \text{Bi}'\left(-\frac{E}{F^{2/3}}\right) + g F^{-1/3} \right] \times \left[2g F^{-2/3} \text{Ai}\left(-\frac{E}{F^{2/3}}\right) \right]^2 \right\} - \left\{ \left[2\pi g F^{-2/3} \text{Bi}\left(-\frac{E}{F^{2/3}}\right) \text{Ai}\left(-\frac{E}{F^{2/3}}\right) - F^{-1/3} \right] \right. \\
&\times \left. \left. \left. \left[(1-g^2)F^{-2/3} \text{Ai}\left(-\frac{E}{F^{2/3}}\right) + \text{Ai}'\left(-\frac{E}{F^{2/3}}\right) \right]^2 \right] \right\} \right). \tag{46}
\end{aligned}$$

The quasibound states correspond to poles of the spectral function, namely solutions to

$$\left[2\pi g F^{-2/3} \text{Ai}\left(-\frac{E}{F^{2/3}}\right) \right]^2 + \left[2\pi g F^{-2/3} \text{Bi}\left(-\frac{E}{F^{2/3}}\right) \text{Ai}\left(-\frac{E}{F^{2/3}}\right) - F^{-1/3} \right]^2 = 0. \tag{47}$$

The real part of the quasienergy can be found by making a perturbative expansion for the real part, E_{real} , of the energy

$$E_{\text{real}} = -g^2 \sum_{n=0}^{\infty} a_n \left(\frac{F}{g^3}\right)^{2n} \tag{48}$$

as in Eq. (34). When the field strength F vanishes, there is a single (even) bound state at $E = -g^2$. Thus, $a_0 = 1$, as is con-

sistent with Eq. (35) when $a \rightarrow 0$. The width of the quasibound state can be estimated by writing

$$E = E_{\text{real}} + iE_{\text{imag}}, \tag{49}$$

where we expect E_{imag} to be exponentially small. Indeed, expanding the imaginary part of Eq. (47) immediately leads to the leading behavior

TABLE I. This table lists the coefficients a_n appearing in the perturbative expansion (48) for the quasienergy level of the atomic system in an electric field. Note that these coefficients are nonalternating in sign, and that their magnitude $N[a_n]$ grows very fast with the perturbative order n , as is shown in the third column. The fourth column shows the ratio of the a_n to the leading factorial growth rate in Eq. (52), and the fifth column gives the fourth-order Richardson extrapolation [46] of this ratio, showing its rapid approach to unity.

n	a_n	$N[a_n]$	$N[a_n/a_n^{(\text{lead})}]$	$R[a_n/a_n^{(\text{lead})}]$
0	1	1		
1	$\frac{5}{16}$	0.3125	0.872665	1.04760
2	$\frac{55}{64}$	0.859	0.71106	0.95104
3	$\frac{10625}{1024}$	10.376	0.763133	0.9533
4	$\frac{1078125}{4096}$	263.214	0.819423	0.98733
5	$\frac{366940625}{32768}$	11198.1	0.860776	1.006199
6	$\frac{93784578125}{131072}$	715520.	0.888895	1.008710
7	$\frac{269028257953125}{4194304}$	6.4×10^7	0.908071	1.005397
8	$\frac{129011616275390625}{16777216}$	7.7×10^9	0.921614	1.002243
9	$\frac{159621687625662109375}{134217728}$	1.2×10^{12}	0.931602	1.000556
10	$\frac{123839968932138228515625}{536870912}$	2.3×10^{14}	0.939271	0.99992
11	$\frac{471147487418797446943359375}{8589934592}$	5.5×10^{16}	0.945356	0.99978
12	$\frac{539212883805702339810673828125}{34359738368}$	1.6×10^{19}	0.950311	0.99981
13	$\frac{14621851148462626262656396484375}{274877906944}$	5.3×10^{21}	0.95443	0.99987
14	$\frac{144871600275431039774199176025390625}{68719476736}$	2.1×10^{24}	0.957911	0.99991
15	$\frac{67969184060037298421788742225469970703125}{70368744177664}$	9.7×10^{26}	0.960894	0.99995
16	$\frac{142608185435906164633493702703533111572265625}{281474976710656}$	5.1×10^{29}	0.963479	0.99997
17	$\frac{679265718819054465192747030828993319061279296875}{2251799813685248}$	3.0×10^{32}	0.965742	
18	$\frac{1822495852683481842017384269925359639728546142578125}{9007199254740992}$	2.0×10^{35}	0.96774	
19	$\frac{21888188031753229357462565895827650045023616790771484375}{144115188075855872}$	1.5×10^{38}	0.969516	
20	$\frac{73105891881984796538857909985635411709301443950653076171875}{576460752303423488}$	1.3×10^{41}	0.971107	

$$E_{\text{imag}} \sim -g^2 \exp\left[-\frac{4g^3}{3F}\right] \quad (50)$$

$$a_n^{(\text{leading})} = \frac{2}{\pi} \left(\frac{3}{4}\right)^{2n} \Gamma(2n). \quad (52)$$

in agreement with the $a \rightarrow 0$ limit of the molecular case (38), and with a simple WKB tunneling estimate.

The perturbative coefficients a_n for the real part of the energy can be generated straightforwardly as follows. First, note that the Ai^2 term in Eq. (47) is exponentially small in the small F limit, and so can be neglected. Thus the real part is determined by

$$\text{Ai}\left[\frac{g^2}{F^{2/3}} \sum_{n=0}^{\infty} a_n \left(\frac{F}{g^3}\right)^{2n}\right] \times \text{Bi}\left[\frac{g^2}{F^{2/3}} \sum_{n=0}^{\infty} a_n \left(\frac{F}{g^3}\right)^{2n}\right] = \frac{F^{1/3}}{2\pi g}. \quad (51)$$

In the small- F limit we can use the asymptotic expansions (31) and (32) of the Airy functions to make an expansion of Eq. (51) in powers of $(F/g^3)^2$, thereby successively determining the coefficients a_n . The results for the first 21 expansion coefficients are shown in Table I.

All the a_n have the same sign, and their magnitude grows factorially fast,

This is in agreement with the tunneling rate and imaginary part (50), using the standard relation between large-order perturbation theory and nonperturbative effects [38–45].

VI. CONCLUSIONS

In this paper, we have presented the exact analytic solution for the spectral function for the simple one-dimensional molecular ionization model of a diatomic molecule represented by two attractive δ -function wells in an external static electric field. The Weyl-Titchmarsh-Kodaira spectral theorem provides a simple construction for the spectral function in terms of suitably normalized solutions to the Schrödinger equation. In this case, these solutions are Airy functions, and the spectral function can be expressed in closed form in terms of Airy functions. Thus, the spectral function can easily be plotted using a program such as Mathematica [37]. The dependence of the spectral function on the relevant physical parameters, the field strength F , the well strength g , and the well separation parameter a , is illustrated in Sec. IV by a collection of plots. This helps develop a body of intuition for the behavior of the quasibound states as they are Stark-shifted and broadened, and also for the resonance structures in the “continuum,” which reflect a competition between

Ramsauer-Townsend resonant scattering between the two atomic wells and between one or both atomic well(s) and the linear field potential. The most important extension of this model would be to consider the effect of time dependence in the background electric field, which introduces yet another physical scale into the problem [47–51].

ACKNOWLEDGMENTS

We thank George Gibson, Misha Ivanov, and Roman Jackiw for helpful comments and suggestions. We also thank Stephen Fulling, Larry Glasser, and Fred Strauch for bringing Refs. [34,30,31,36] to our attention.

-
- [1] K. Codling, L. J. Frashinski, and P. A. Hatherly, *J. Phys. B* **22**, L321 (1989); J. H. Posthumus, K. Codling, L. J. Frashinski, and M. R. Thompson, *Laser Phys.* **7**, 813 (1997).
- [2] R. R. Freeman and P. H. Bucksbaum, *J. Phys. B* **24**, 325 (1991).
- [3] J. P. Nibarger, S. V. Menon, and G. N. Gibson, *Phys. Rev. A* **63**, 053406 (2001).
- [4] P. B. Corkum, N. H. Burnett, and F. Brunel, *Phys. Rev. Lett.* **62**, 1259 (1989); P. B. Corkum, *ibid.* **71**, 1994 (1993).
- [5] P. Hansch, M. A. Walker, and L. D. Van Woerkom, *Phys. Rev. A* **55**, R2535 (1997).
- [6] B. Walker, B. Sheehy, L. F. DiMauro, P. Agostini, K. J. Schafer, and K. C. Kulander, *Phys. Rev. Lett.* **73**, 1227 (1994).
- [7] A. D. Bandrauk and H. Yu, *Phys. Rev. A* **59**, 539 (1999).
- [8] P. Dietrich, D. T. Strickland, M. Laberge, and P. B. Corkum, *Phys. Rev. A* **47**, 2305 (1993); I. V. Litvinyuk, K. F. Lee, P. W. Dooley, D. M. Rayner, D. M. Villeneuve, and P. B. Corkum, *Phys. Rev. Lett.* **90**, 233003 (2003).
- [9] T. Seideman, M. Yu. Ivanov, and P. B. Corkum, *Phys. Rev. Lett.* **75**, 2819 (1995); M. Ivanov, T. Seideman, P. Corkum, F. Ilkov, and P. Dietrich, *Phys. Rev. A* **54**, 1541 (1996).
- [10] A. Talebpour, S. Larochelle, and S. L. Chin, *J. Phys. B* **30**, L245 (1997).
- [11] G. Gibson, T. S. Luk, A. McPherson, K. Boyer, and C. K. Rhodes, *Phys. Rev. A* **40**, 2378 (1989).
- [12] M. Schmidt, D. Normand, and C. Cornaggia, *Phys. Rev. A* **50**, 5037 (1994).
- [13] A. Talebpour, C.-Y. Chien, and S. L. Chin, *J. Phys. B* **29**, L677 (1996).
- [14] R. Barnett and G. N. Gibson, *Phys. Rev. A* **59**, 4843 (1999).
- [15] P. Froelich and E. Brändas, *Phys. Rev. A* **12**, 1 (1975).
- [16] S. Geltman, *J. Phys. B* **11**, 3323 (1978).
- [17] W. P. Reinhardt, *Int. J. Quantum Chem., Symp.* **10**, 359 (1976).
- [18] T. Yamabe, A. Tachibana, and H. J. Silverstone, *Phys. Rev. A* **16**, 877 (1977); *J. Phys. B* **10**, 2083 (1977).
- [19] M. V. Ammosov, N. B. Delone, and V. P. Krainov, *Sov. Phys. JETP* **64**, 1191 (1986).
- [20] See, for example, S. Gasiorowicz, *Quantum Physics* (Wiley, New York, 2003).
- [21] Yu. N. Demkov and V. N. Ostrovskii, *Zero-Range Potentials and their Applications in Atomic Physics* (Plenum, New York, 1988).
- [22] H. Weyl, *Math. Ann.* **68**, 220 (1910).
- [23] E. C. Titchmarsh, *Eigenfunction Expansions Associated with Second-Order Differential Equations, Vols. I and II* (Oxford University Press, Oxford, 1946); *Proc. R. Soc. London, Ser. A* **207**, 321 (1951).
- [24] K. Kodaira, *Am. J. Math.* **71**, 921 (1949).
- [25] R. D. Richtmyer, *Principles of Advanced Mathematical Physics* (Springer, New York, 1978).
- [26] M. Hehenberger, H. V. McIntosh, and E. Brändas, *Phys. Rev. A* **10**, 1494 (1974).
- [27] C. E. Dean and S. A. Fulling, *Am. J. Phys.* **50**, 540 (1982).
- [28] G. N. Gibson, G. V. Dunne, and K. J. Bergquist, *Phys. Rev. Lett.* **81**, 2663 (1998).
- [29] E. Y. Sidky and I. Ben-Itzhak, *Phys. Rev. A* **60**, 3586 (1999).
- [30] M. L. Glasser, W. Jaskólski, F. García-Moliner, and V. R. Velasco, *Phys. Rev. B* **42**, 7630 (1990).
- [31] H. J. Korsch and S. Mossmann, *J. Phys. A* **36**, 2139 (2003).
- [32] *Handbook of Mathematical Functions*, edited by M. Abramowitz and I. A. Stegun (Dover, New York, 1998).
- [33] Animations of the spectral function dependence on the physical parameters F , a , and g can be found at <http://www.phys.uconn.edu/~dunne/starkanimations/SpecMovies.html>.
- [34] A. Ludviksson, *J. Phys. A* **20**, 4733 (1987).
- [35] R. M. Cavalcanti, P. Giacconi, and R. Soldati, *J. Phys. A* **36**, 12065 (2003).
- [36] G. Alvarez and B. Sundaram, *Phys. Rev. A* **68**, 013407 (2003).
- [37] S. Wolfram, *MATHEMATICA 5* (2003).
- [38] A. I. Vainshtein, *Decaying Systems and Divergence of Perturbation Theory*, Novosibirsk Report, 1964, reprinted in Russian, with an English translation by M. Shifman, in *ArkadyFest 2002, Continuous advances in QCD*, edited by K. A. Olive *et al.* (World Scientific, Singapore, 2002).
- [39] C. M. Bender and T. T. Wu, *Phys. Rev.* **184**, 1231 (1969); *Phys. Rev. Lett.* **27**, 461 (1971); *Phys. Rev. D* **7**, 1620 (1973).
- [40] *Large-Order Behaviour of Perturbation Theory*, edited by J. C. Le Guillou and J. Zinn-Justin (North Holland, Amsterdam, 1990).
- [41] G. V. Dunne, *Perturbative-nonperturbative Connection in Quantum Mechanics and Field Theory*, in *Proceedings of ArkadyFest 2002* (Ref. [38]), pp 478–505.
- [42] H. J. Silverstone, *Phys. Rev. A* **18**, 1853 (1978).
- [43] V. Franceschini, V. Grecchi, and H. J. Silverstone, *Phys. Rev. A* **32**, 1338 (1985).
- [44] I. A. Ivanov, *Phys. Rev. A* **56**, 202 (1997).
- [45] U. D. Jentschura, *Phys. Rev. A* **64**, 013403 (2001).
- [46] C. M. Bender and S. A. Orszag, *Advanced Mathematical Methods for Scientists and Engineers* (McGraw-Hill, New York, 1978).
- [47] L. V. Keldysh, *Sov. Phys. JETP* **20**, 1307 (1964).
- [48] S. Geltman, *J. Phys. B* **10**, 831 (1977).
- [49] H. R. Reiss, *Phys. Rev. A* **22**, 1786 (1980).
- [50] S.-I. Chu, *Adv. At. Mol. Phys.* **21**, 197 (1985).
- [51] M. V. Frolov, N. L. Manakov, E. A. Pronin, and A. F. Starace, *Phys. Rev. Lett.* **91**, 053003 (2003).